A way to increase parabolic trough plant yield by roughly 2% using all sky imager derived DNI maps

Cite as: AIP Conference Proceedings **2303**, 110005 (2020); https://doi.org/10.1063/5.0028667
Published Online: 11 December 2020

Bijan Nouri, Kareem Noureldin, Tim Schlichting, Stefan Wilbert, Tobias Hirsch, Marion Schroedter-Homscheidt, Pascal Kuhn, Andreas Kazantzidis, Luis F. Zarzalejo, Philippe Blanc, Zeyad Yasser, Jesús Fernández, and Robert Pitz-Paal

A Way to Increase Parabolic Trough Plant Yield by Roughly 2% Using All Sky Imager Derived DNI Maps

Bijan Nouri[1, a)], Kareem Noureldin[2], Tim Schlichting[3], Stefan Wilbert[1], Tobias Hirsch[2], Marion Schroedter-Homscheidt[4], Pascal Kuhn[1], Andreas Kazantzidis[5], Luis F. Zarzalejo[6], Philippe Blanc[7], Zeyad Yasser[8], Jesús Fernández[9] and Robert Pitz-Paal[10]

[1]*German Aerospace Center (DLR), Institute of Solar Research, Ctra de Senes s/n km 4, 04200 Tabernas, Spain*
[2]*German Aerospace Center (DLR), Institute of Solar Research, Wankelstrasse 5, 70563 Stuttgart, Germany*
[3]*German Aerospace Center (DLR), Institute of Solar Research, Solar Power Plant Technology, Prof.-Rehm-Str. 1, 52428 Jülich, Germany*
[4]*German Aerospace Center (DLR), Institute of Networked Energy Systems, Carl-von-Ossietzky-Straße 15, 26129 Oldenburg, Germany*
[5]*Laboratory of Atmospheric Physics, Department of Physics, University of Patras, 26500 Patras, Greece*
[6]*CIEMAT Energy Department – Renewable Energy Division, Av. Complutense 40, 28040 Madrid, Spain*
[7]*MINES ParisTech, 06904 Sophia Antipolis CEDEX, France*
[8]*TSK Flagsol Engineering GmbH, Anna-Schneider-Steig 10, 50678 Cologne, Germany*
[9]*CIEMAT-Plataforma Solar de Almería, Ctra. de Senés km 4.5, E-04200 Tabernas, Almería, Spain*
[10]*DLR, Institute of Solar Research, Linder Höhe, 51147 Cologne, Germany*

[a)]Corresponding author: bijan.nouri@dlr.de

Abstract. Solar fields of parabolic troughs are extensive complex thermal hydraulic facilities. Intra-hour and intra-minute variabilities of the DNI, mainly caused by passing clouds, pose an operational challenge for parabolic trough power plants. Under perfect circumstances a solar field controller would adjusts the mass flow in such a way, that the design temperature is always maintained constant with a maximized focus rate. However, heterogeneous irradiance conditions or flow distribution may cause some solar field sections to temporarily overheat while others may not reach the set point temperature, which in turn leads to an economic loss. State of the art solar field controllers have only access to incomplete information on spatial DNI variability, from DNI measurements of few pyrheliometers. Solar field controllers could be optimized with access to highly resolved DNI informations both in space and time. Such DNI information can be provided by all sky imager (ASI) based irradiance monitoring systems. In a previous study we developed and benchmarked new solar field controllers with access to spatial DNI information from an ASI system for a 50 MWe plant close to Córdoba (Spain). Significant improvements in revenue were observed. Yet, this previous study was limited to 22 days only. In this study, we estimate the potential benefit of these new solar field controllers over a 2 year period on the basis of the simulation results over 22 days. The upscaling method makes use of DNI variability classes. Using the ASI data we obtain a significant improvement in revenue up to 2% for the 2 year period.

INTRODUCTION

Parabolic trough (PT) power plants with thermal energy storages (TES) provide a dispatchable and renewable energy source for regions with a high annual direct normal irradiance (DNI) sum. Therefore, PT power plants could play a vital balancing role in electrical grids with an increased share of intermittent sources such as solar photovoltaic or wind [1]. Whether we will see a continuous growth of the global PT power plant industry depends predominantly on the economic competitiveness against other renewable or conventional technologies. Significant

SolarPACES 2019
AIP Conf. Proc. 2303, 110005-1–110005-10; https://doi.org/10.1063/5.0028667
Published by AIP Publishing. 978-0-7354-4037-1/$30.00

reductions in levelized cost of electricity (LCoE) were reached in the last couple of years [2]. Yet, PT power plants still offer a considerable cost reduction potential, mainly by scale effects, by improving the component efficiencies or by optimizing the plant operation [3]. This work contributes to the optimization of the plant operation.

PT solar fields are complex and extensive thermal hydraulic facilities, which concentrate the DNI on receiver tubes and pass the energy to a heat transfer fluid which in turn passes the energy to a conventional Rankine cycle or a TES. A perfect solar field controller adjusts the mass flow in such a way, that the design temperature is always maintained constant without any need of defocusing collectors. Particularly under variable conditions, mainly caused by passing clouds with spatially heterogeneous optical thickness, the solar field controllers cannot meet this ideal control scenario. State of the art controllers only have access to the DNI signal from few pyrheliometers, and thus have only limited information on spatial variability of the DNI. Better information on spatially distributed DNI over the extensive solar field could help to improve control processes under variable conditions. Camera based monitoring systems can provide DNI information with a high spatial and temporal resolution, which allows an analysis of the spatial and temporal variability of the DNI in space and time.

Distinct camera based monitoring systems are described in the literature, some consist of upward-facing all sky imagers (ASI) [4-6] other consist of downward-facing shadow cameras [7]. Where ASI based systems detect clouds in the sky and project there shadows on the ground, detect shadow camera based systems directly shadows on the ground. Both approaches can convert shadow maps into irradiance maps with access to local irradiance measurements.

Comprehensive numerical models are suitable for the development and qualification of new control strategies [8-12]. [12] developed a simulation environment for entire PT solar fields called virtual solar field (VSF), which can consider spatially inhomogeneous DNI informations from camera based monitoring systems.

The fundamental potential of spatial DNI information for the optimization of PT solar field controller was investigated with the VSF by [13], showing a potential gain in revenue up to 2.5% for some days. However, this study did not consider the uncertainties of the spatial DNI information from a camera based monitoring systems. A follow-up study [14] developed and evaluated the potential benefit of PT solar field controllers with access to DNI maps from an ASI system [6], under consideration of the ASI systems uncertainties by incorporating additional spatial DNI information from an shadow camera system [7]. Both involved camera based monitoring systems are operated at CIEMAT's Plataforma Solar de Almería (PSA). [14] does not use the spatial DNI information for the control of the individual solar field collectors directly, knowing that the uncertainties might be considerably high at any given moment and for any discrete spot of the solar field. Instead, in indirect approach is used in which the spatial and temporal DNI variability at any given moment is classified using the DNI maps. The classification results as well as the average DNI over the solar field are handed to the PT solar field controller. Optimized specific control parameters are presented in [14] for each of the spatial and temporal DNI variability classes. These new class dependent control strategies were benchmarked against a state of the art parabolic trough solar field controller. The benchmarking comprised 22 days, with a wide variety of conditions in irradiance, cloud height and type (low layer, middle layer, high layer and multi-layer conditions) as well as the resulting DNI variability classes. An overall increase in revenue by roughly 2% was observed. The DNI classification procedure was crucial for this significant improvement, as the used camera based monitoring systems are capable to catch the prevailing overall spatial and temporal DNI variability conditions accurately enough for the plant control, despite the significant uncertainties of the spatial DNI information.

In this study we investigate the potential benefit of these new DNI variability class dependent controllers over two entire years (2016 and 2017). Performing a 2 year study with VSF and shadow camera data is not feasible due to limit available shadow camera data and calculation time. Therefore, no VSF simulations are performed. Instead we developed a statistical approach to estimate the influence of the new controllers. This approach utilizes the relative change in revenue of the class dependent controller compared to a state of the art controller of the previous 22 days obtained for combinations of spatial and temporal DNI variability classes. These values of relative change in revenue are treated as expected relative change in revenue for the corresponding DNI variability class combinations. For the estimation, we analyze the distribution of prevailing DNI variability class combinations for each day.

In the following sections we will briefly present the used results of the previously published study before we describe the estimation procedure in more detail. Finally we will summarize our findings and present an outlook.

RESULTS OF VSF SIMULATIONS WITH CLASS DEPENDENT CONTROLLERS

This section summarizes some results of the study [14], which are the basis of the statistical approach for the benefit estimation of the class dependent controller over a two year period, as presented in the following section.

Spatial and Temporal DNI Variability Classification

Two distinct DNI variability classification procedures are utilized. The temporal DNI variability classification describes the temporal variability as observed by a pyrheliometer [15,16] whereas the spatial DNI variability describes the spatial heterogeneity of DNI on the solar field as observed by the ASI system [14].

The DNI conditions are classified into 8 temporal and 5 spatial classes (see Table 1). Figure 1 shows the DNI, clear sky DNI and the corresponding temporal as well as spatial DNI variability classification for the 09.09.2015 and PSA as an example. The conditions show a low variability in time and space until 11 UTC, afterwards the variabilities in DNI increase induced by passing clouds. Despite the variable conditions the DNI remains mostly at a considerably high level above 400 W/m².

TABLE 1. Description temporal and spatial DNI variability classes

Class	General description temporal DNI variability	General description spatial DNI variability
1	Clear sky conditions with low temporal DNI variability and very high clear sky index	Sunny conditions on solar field
2	Almost clear sky with low temporal DNI variability and high clear sky index	Low spatial DNI variability: Only shadows from clouds with high transmittance
3	Almost clear sky with intermediate temporal DNI variability and high/ intermediate clear sky index	High spatial DNI variability
4	Partly cloudy with high temporal DNI variability and intermediate clear sky index	Intermediate spatial variability: Most of the solar field shaded Cases with only thin clouds and only thick clouds excluded
5	Partly cloudy with intermediate temporal DNI variability and intermediate clear sky index	Low spatial variability: Most of the solar field shaded (overcast) Only shadows from clouds with low transmittance
6	Partly cloudy with high temporal DNI variability and intermediate/low clear sky index	-
7	Almost overcast with intermediate temporal DNI variability and low clear sky index	-
8	Overcast with low temporal DNI variability and very low clear sky index	-

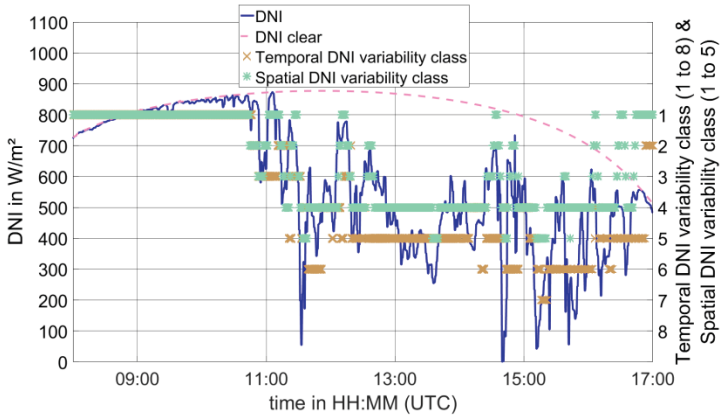

FIGURE 1. Spatial DNI variability classes of an example day (09.09.2015)

Reference and Class Dependent Controllers

The class dependent controllers and the state of the art reference controller utilized by [14] are tailored to the La Africana solar field design. La Africana is a commercial 50 MW PT power plant operated in southern Spain. [14] developed two distinct class dependent control strategies with optimized controller parameters for distinct combinations of spatial and temporal DNI variabilities [17]. These control strategies are called objective temperature (OT) and objective focus rate (OFR). The OT controller is trimmed to maintain the solar field outlet temperature as constant as possible, whereas the OFR controller tries to maximize the solar heat collection by minimizing any defocusing. Whereas the class dependent controller have access to the spatial DNI information from the ASI system has the reference controller only access to DNI measurements from two pyrheliometers, according to the La Africana power plant.

Results of VSF Simulations with Class Dependent Controllers

The two novel class dependent controllers were benchmarked over 22 days with the state of the art controller. For the simulations the novel class dependent controllers receive the expected average DNI on the solar field and the corresponding variability classification results determined from DNI maps created by the ASI system described in [6]. The actual ruling DNI conditions acting on the solar field are provided by a shadow camera system [7]. Both camera systems are operated contemporaneous at PSA. By utilizing two distinct sources for the DNI maps, it is possible to evaluate the solar field operation, considering that the ASI derived DNI maps seen by the controllers are different compared to the actual DNI conditions.

Overall the class dependent controllers outperformed the reference controller by 1.38% (OT controller) and 1.4% (OFR controller) in terms of revenue. The monetary assessment of PT solar field controller with the results of VSF simulations are carried out according to the procedures described in [13].

Eight temporal and five spatial DNI variability classes result in 40 possible combinations. Table 2 shows the change in relative revenue and relative occurrence of combination between spatial and temporal DNI variability discretized over the combinations. Nine of the 40 combinations do not occur within the 22 day benchmarking campaign. The class dependent controllers outperform the reference controller in 20 (OT) and 22 (OFR) combinations of spatial and temporal DNI variability conditions (green cells) which make more than 85% (OT) and 89% (OFR) of the data set. Almost all conditions with an advantage for the reference controller are found for highly variable or overcast conditions, which are not frequent and connected to a low average DNI and plant yield. Some combinations show very pronounced double digit changes in relative revenue. All these combinations are linked to rare transient conditions with an occurrence <0.1% of the data set. For most of the remaining combinations the change in relative revenue is within ±5%.

TABLE 2. Change in relative revenue (upper value in each cell; positive values indicate an improvement compared to the reference controller) and relative occurrence of combination between spatial and temporal DNI variability (lower value in each cell) discretized in combinations of temporal and spatial DNI variability classes (left) OT controller (right) OFR controller

Spatial DNI variability class 1 to 5	Temporal DNI variability class 1 to 8							
	1	2	3	4	5	6	7	8
5	-	-	27.5% <0.1%	-3.6% 0.49%	3.2% 0.14%	-2.2% 3.06%	0.5% 3.73%	5.9% 0.96%
4	-	-2.0% 0.10%	0.3% 0.49%	0.7% 2.86%	-2.7% 2.09%	-0.1% 4.11%	-8.5% 0.61%	-
3	13.9% <0.1%	1.4% 0.36%	0.3% 2.84%	0.1% 3.15%	-3.0% 0.85%	-3.9% 2.10%	-18.4% <0.1%	-
2	2.2% 0.27%	0.7% 0.84%	0.9% 1.80%	0.4% 0.84%	0.7% 0.71%	-7.1% 0.31%	-	-
1	1.0% 47.10%	2.1% 13.98%	3.1% 2.96%	-1.6% 1.02%	1.9% 1.78%	1.4% 0.23%	-	-

Spatial DNI variability class 1 to 5	Temporal DNI variability class 1 to 8							
	1	2	3	4	5	6	7	8
5	-	-	30.5% <0.1%	-4.5% 0.49%	-6.8% 0.14%	-2.7% 3.06%	-2.2% 3.73%	0.5% 0.96%
4	-	0.1% 0.10%	1.2% 0.49%	1.1% 2.86%	-6.6% 2.09%	3.9% 4.11%	-8.9% 0.61%	-
3	16.7% <0.1%	0.3% 0.36%	0.8% 2.84%	1.8% 3.15%	0.1% 0.85%	0.7% 2.10%	-21.2% <0.1%	-
2	-3.1% 0.27%	0.1% 0.84%	2.5% 1.80%	3.2% 0.84%	1.8% 0.71%	-8.2% 0.31%	-	-
1	0.8% 47.10%	2.1% 13.98%	3.7% 2.96%	0.1% 1.02%	3.1% 1.78%	1.0% 0.23%	-	-

[14] utilizes the results depicted in Table 2 as binary decision system for the applicability of the class dependent controller. From this, a hybridized solar field controller concept was developed, which consists of two sets of controllers. The first one is the reference controller making use of the irradiance information from two pyrheliometers whereas the second one uses the class dependent control parameters with access to the ASI system. The class dependent controller are considered as applicable when the DNI conditions correspond to a combination of spatial and temporal DNI variability class with an expected positive relative change in revenue (green cells Table 2).

A clear improvement is visible for the hybridized control concept (see Table 3). The hybridized controllers outperform the reference controller in shares of 91.0% (OT hybridized) or 96.8% (OFR hybridized) of the entire data set, with an overall benefit of 1.93% (OT hybridized) or 1.95% (OFR hybridized) in revenue.

TABLE 3. Change in relative revenue (upper value in each cell; positive values indicate an improvement compared to the reference controller) and relative occurrence of combination between spatial and temporal DNI variability (lower value in each cell) discretized in combinations of temporal and spatial DNI variability classes (left) OT hybridized controller (right) OFR hybridized controller

Spatial DNI variability class 1 to 5	Temporal DNI variability class 1	2	3	4	5	6	7	8
5	-	-	27.2% <0.1%	-4.0% 0.49%	9.0% 0.14%	-1.8% 3.06%	-2.1% 3.73%	1.7% 0.96%
4	-	-0.3% 0.10%	1.2% 0.49%	0.2% 2.86%	7.2% 2.09%	3.0% 4.11%	-5.5% 0.61%	-
3	13.5% <0.1%	1.4% 0.36%	1.6% 2.84%	2.0% 3.15%	2.0% 0.85%	2.6% 2.10%	0.5% <0.1%	-
2	2.9% 0.27%	4.7% 0.84%	2.9% 1.80%	3.7% 0.84%	4.5% 0.71%	4.5% 0.31%	-	-
1	1.2% 47.10%	3.3% 13.98%	2.1% 2.96%	-1.0% 1.02%	2.9% 1.78%	2.2% 0.23%	-	-

Spatial DNI variability class 1 to 5	Temporal DNI variability class 1	2	3	4	5	6	7	8
5	-	-	31.8% <0.1%	-2.3% 0.49%	16.0% 0.14%	5.6% 3.06%	1.5% 3.73%	4.2% 0.96%
4	-	-1.1% 0.10%	1.5% 0.49%	3.0% 2.86%	7.7% 2.09%	8.2% 4.11%	-2.7% 0.61%	-
3	16.4% <0.1%	0.1% 0.36%	1.4% 2.84%	2.9% 3.15%	0.0% 0.85%	3.1% 2.10%	-0.4% <0.1%	-
2	2.9% 0.27%	0.9% 0.84%	2.1% 1.80%	2.5% 0.84%	1.7% 0.71%	0.3% 0.31%	-	-
1	1.0% 47.10%	2.9% 13.98%	3.3% 2.96%	-0.6% 1.02%	2.5% 1.78%	2.5% 0.23%	-	-

The values of relative change in revenue for distinct combinations of spatial and temporal DNI variability classes depicted in Table 3 are the basis of this study. In the subsequent section the potential benefit of the new solar field controllers is estimated by means of a statistical approach over a two year period.

PERFORMANCE ESTIMATION OF CLASS DEPENDENT CONTROL STRATEGIES OVER A 2 YEAR PERIOD

Based on the detailed evaluation over 22 days, the impact of the new control strategies is estimated over the years 2016 and 2017 at PSA. Only the superior hybridized control concepts with regards to the applicability conditions are considered for this study. For the performance estimation the distribution of the occurred combinations of temporal and spatial DNI variability is analyzed individually for each day of the years 2016 and 2017.

The distribution for a given day is described as $f_{iD,iC}$ for the combinations iC =1…40. The overall expected relative change in revenue per day ($c_{rel.rev,est,iD}$) is estimated by combining $f_{iD,iC}$ with the expected relative change in revenue for the corresponding class combinations ($c_{rel.rev,exp,iC}$) from Table 3:

$$c_{rel.rev,est,iD} = \sum_{iC=1}^{nC=40} f_{iD,iC} \cdot c_{rel.rev,exp,iC} \quad (1)$$

The distribution of all occurred combinations over the years 2016 and 2017 at PSA is listed in Table 4. Only roughly 0.4% of the two year data set corresponds to DNI variability conditions which did not occur within the 22 day benchmarking campaign. These conditions are not taken into account for the estimation procedure. The energetic effect of these conditions is marginal for PT power plant operation, as they belong to overcast transient conditions.

TABLE 4. Temporal and spatial DNI variability class distribution of possible combinations within the years 2016 and 2017.

Spatial DNI variability class 1 to 5	1	2	3	4	5	6	7	8
5	0.30%	0%	<0.1%	0.12%	0.27%	2.35%	6.42%	6.11%
4	<0.1%	<0.1%	0.29%	1.07%	2.71%	3.36%	1.04%	<0.1%
3	0.10%	0.26%	1.16%	1.50%	0.81%	1.03%	<0.1%	<0.1%
2	0.32%	1.02%	1.04%	0.47%	0.67%	0.19%	<0.1%	0%
1	43.53%	19.44%	2.04%	0.53%	1.56%	0.16%	<0.1%	0%

Temporal DNI variability class 1 to 8

The distribution of change in relative revenue over all days is shown in Fig. 2. We see a positive benefit in 94.8% (OT hybridized) and 99.9% (OFR hybridized) of all days. Both controllers show the highest day count for a change in relative revenue of roughly 1.4%. Min, max and some selected percentile values corresponding to the 2 year data set are shown in Fig. 3. From Fig. 3 we see that the OFR hybridized controller outperforms the OT hybridized controller in all percentile ranges.

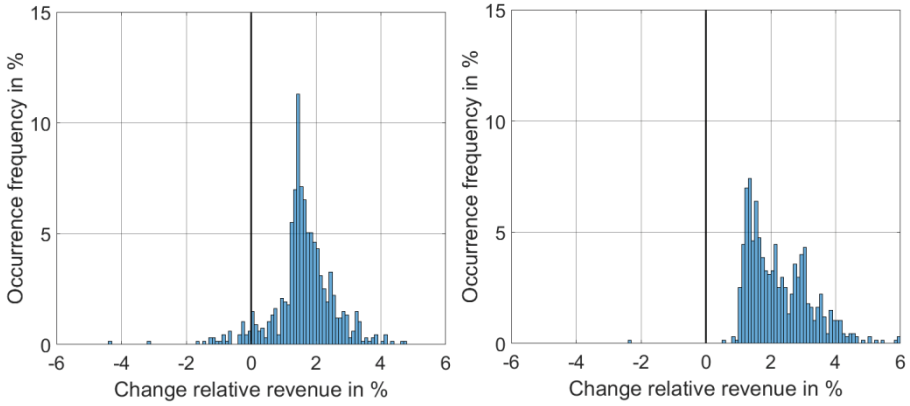

FIGURE 2. Distribution of change in relative revenue per day between class dependent controllers and reference controller over the years 2016 and 2017 with regards to the applicability conditions (left) OT hybridized (right) OFR hybridized

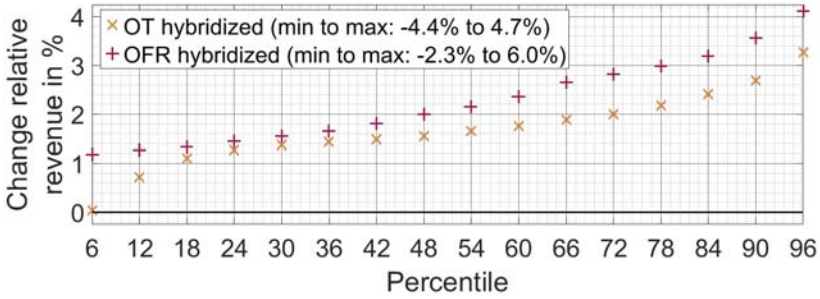

FIGURE 3. Min, max and some selected percentile values of estimated change in relative revenue over all days (hybridized controller)

That the OFR hybridized controller outperforms the OT hybridized controller can be explained by the used data sets and the previously determined expected relative change in revenue within distinct combinations of spatial and temporal DNI variability classes. Only 6 combinations for both controllers remain, for which the reference controller outperforms the corresponding class dependent controller (see Table 3). For the OFR hybridized controller the 6 combinations are evenly distributed over distinct variability conditions, which explains why the OFR hybridized controller outperforms the reference controller on almost all days. On the contrary the OT hybridized controller is outperformed by two overcast conditions (spatial class 5 and temporal class 6 to 7), which makes the OT hybridized controller less suitable during days with continuous overcast conditions.

Of course we should always take into account that not all days have the same contribution to the overall plant yield. Figure 4 illustrates the estimated change in relative revenue per day over the corresponding daily effective DNI sum. The effective DNI is calculated according to

$$DNI_{eff} = DNI \cdot \cos(\theta) \tag{2}$$

with θ as the incidence angle on the PT collectors. The incidence angle of a PT collector in north south alignment can be calculated according to

$$\theta = \operatorname{acos}\left(\sqrt{cos^2(\theta_z) + cos^2(\delta) \cdot sin^2(\omega)}\right) \tag{3}$$

with θ_z as solar zenith angle, δ as declination and ω as hour angle [18]. It is clearly visible that both class dependent controllers work well on days with a high daily effective DNI sum. Around 91% of all days with an negative benefit for the OT hybridized controller belong to days with a low daily effective DNI sum <2 kWh/(m²day), which corresponds to the previously mentioned weaknesses of the OT hybridized controller with predominantly overcast days.

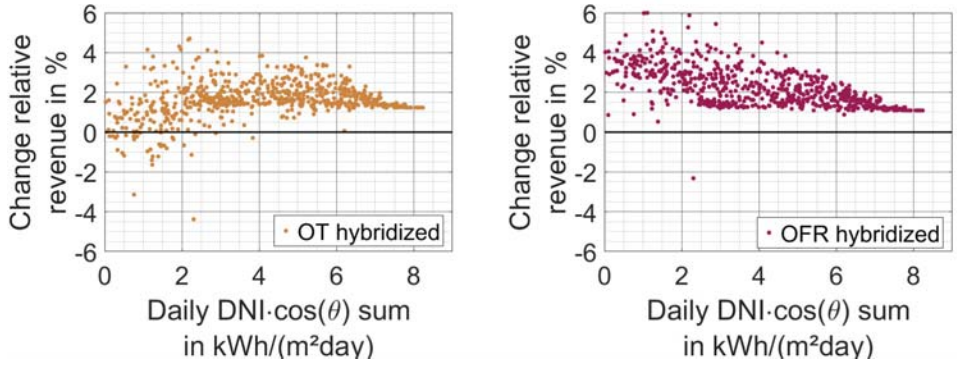

FIGURE 4. Estimated change relative revenue per day over daily effective DNI sum (hybridized controller)

Weighted average values of the change in relative revenue over distinct ranges of daily effective DNI sum ($c_{rel.rev,est,range}$) are shown in Fig. 5. Figure 5 also includes the corresponding distribution of the daily sums of DNI_{eff}. The weighting factor of each day is based on the quotient of the daily effective DNI sum and the effective DNI sum over all days within that range, according to equation 4

$$c_{rel.rev,est,range} = \frac{\sum_{iD}^{nD} c_{rel.rev,est,iD} \cdot \frac{DNI_{eff,iD}}{DNI_{eff,range}}}{nD}, \tag{4}$$

where nD is the total number of all days within a particular range. The weighted average changes in relative revenue within distinct ranges of daily effective DNI sum show a similar benefit for both controllers in days with a daily effective DNI sum above 3 kWh/(m²day). In fact, a small advantage of the OT hybridized controller is visible for these ranges. In contrast, a significant advantage of the OFR hybridized controller is visible for days with a daily effective DNI sum below 3 kWh/(m²day). Over all days the weighted average change in relative revenue amounts to 1.8% (OT hybridized) and 2.0% (OFR hybridized) respectively. The estimated improvement of 2.0% in revenue corresponds in the case of La Africana to 2.0 GWh/year or roughly 200,000 €/year.

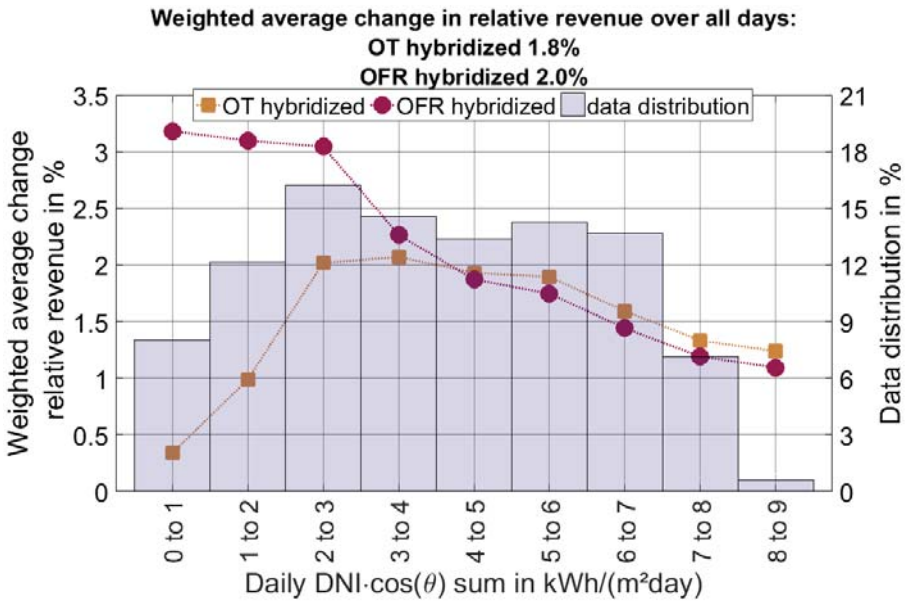

FIGURE 5. Weighted average change relative revenue over all days within distinct ranges of Daily effective DNI sum as well as corresponding data distribution (hybridized controller)

CONCLUSION

In this study we evaluated the potential benefit of spatial DNI information from ASI systems over a period of two complete years (2016 and 2017). Parabolic trough (PT) solar field controllers with access to spatial DNI information were developed in a previous study [14]. These so called class dependent controller utilize optimized specific control parameters for distinct combinations of spatial and temporal DNI variability classes, as classified from the ASI systems DNI maps. The uncertainties of the ASI system were considered, by introducing additional spatial DNI information from a fundamentally distinct shadow camera system, which describes the real weather conditions unknown by the solar field controllers.

[14] benchmarked over 22 days two distinct control strategies (OT: Objective temperature and OFR objective focus rate) as well as a hybridized controller for PT solar fields. The hybridized control concept decides at any point in time between the class dependent controller or a state of the art controller, according to the prevailing DNI variability conditions and the results of an applicability analysis. From the benchmark the expected change in revenue within possible combinations of spatial and temporal DNI variability classes for the hybridized controller are known.

For this study, the distribution of occurring spatial and temporal DNI variability combinations for each day within the years 2016 and 2017 were analyzed. Subsequently, these distributions were combined with the expected change in revenue of the hybridized controller within the combinations, which leads to an estimate of the expected change in revenue per day. We see that the hybridized controllers lead to a benefit in 94.8% (OT hybridized) and 99.9% (OFR hybridized) of the days. Looking into the daily effective DNI sum, it is clear that almost all days were the state of the art controller outperforms the hybridized controllers belong to energetically less interesting days (daily effective DNI sum <2 kWh/(m²day)). In average over all days of the two years the plant revenue increases significantly by 1.8% (OT hybridized) and 2.0% (OFR hybridized) compared to a state of the art controller.

It has to be considered that the ASI system provides also predictions up to 15 minutes ahead. However, currently the predictions are not utilized by the investigated power plant controller. A further improvement could be achieved by including model predictive control strategies, which could utilize the predictions.

All controller used in this study are tailored to the La Africana solar field design. Nevertheless, similar possible improvements are expected for other PT power plants. Even power plants with fundamentally different control approaches can benefit from the spatial DNI information with the associated spatial and temporal DNI variability classes, as these are additional input information which can be introduced to any existing or future PT solar field controller.

Finally, we would like to mention that other CSP technologies, such as Fresnel and point focusing tower power plants, could also benefit from the spatial DNI information provided by ASIs.

ACKNOWLEDGMENTS

Funding was received by the German Federal Ministry for Economic Affairs and Energy within the WobaS-A project (Grant Agreement 0324307A).

Thanks to the colleagues from the Solar Concentrating Systems Unit of CIEMAT for the support provided in the installation and maintenance of the shadow cameras. These instruments are installed on CIEMAT's CESA-I tower of the Plataforma Solar de Almería.

REFERENCES

1. Mehos, M., Turchi, C., Jorgenson, J., Denholm, P., Ho, C. and Armijo, K. On the Path to SunShot: Advancing Concentrating Solar Power Technology, Performance, and Dispatchability. Golden, CO: National Renewable Energy Laboratory. NREL/TP-5500-65688 (2016). http://www.nrel.gov/docs/fy16osti/65688.pdf.
2. Lilliestam, J. and Pitz-Paal, R. Concentrating solar power for less than USD 0.07 per kWh: finally the breakthrough?. Renewable Energy Focus, 26:17-21 (2018). doi: 10.1016/j.ref.2018.06.002
3. Pitz-Paal, R. Concentrating solar power: still small but learning fast. Nature Energy. 2(7):17095 (2017). doi: 10.1038/nenergy.2017.95
4. Blanc, P., Massip, P., Kazantzidis, A., Tzoumanikas, P., Kuhn, P., Wilbert, S., Schüler, D. and Prahl, C. Short-Term Forecasting of High Resolution Local DNI Maps with Multiple Fish-Eye Cameras in Stereoscopic Mode, AIP conference Proceedings 1850 (2017). doi: 10.1063/1.4984512
5. Kazantzidis, A., Tzoumanikas, P., Blanc, P., Massip, P., Wilbert, S. and Ramirez-Santigosa, L. Short-term forecasting based on all-sky cameras, In: Renewable Energy Forecasting. Woodhead Publishing Series in Energy. Woodhead Publishing, pp. 153–178 (2017). doi: 10.1016/B978-0-08-100504-0. 00005-6.
6. Nouri, B., Wilbert, S., Segura, L., Kuhn, P., Hanrieder, N., Kazantzidis, A., Schmidt, T., Zarzalejo, L., Blanc, P. and Pitz-Paal, R. Determination of cloud transmittance for all sky imager based solar nowcasting. Sol. Energy, 181, 251–263 (2019). doi: 10.1016/j.solener.2019.02.004.
7. Kuhn, P., Wilbert, S., Prahl, C., Schüler, D., Haase, T., Hirsch, T., Wittmann, M., Ramirez, L., Zarzalejo, L., Meyer, A. and Vuilleumier, L. Shadow camera system for the generation of solar irradiance maps. Sol. Energy 157, 157–170 (2017). doi: 10.1016/j.solener.2017.05.074
8. Hirsch, T. and Schenk, HE. Dynamics of oil-based parabolic trough plants—A detailed transient simulation model. In Proceedings of the SolarPACES 2010 Conference, Perpignan (France)
9. García, I., Álvarez, J. and Blanco, D. Performance model for parabolic trough solar thermal power plants with thermal storage: comparison to operating plant data. Sol. Energy 95, 2443–2460 (2011). doi: 10.1016/j.solener.2011.07.002
10. Giostri, A.Transient effects in linear concentrating solar thermal power plant, Ph.D. thesis, Energy Department, Politecnico Di Milano (2012). http://hdl.handle.net/10589/89590
11. Zaversky, F., Medina, R., García-Barberena, J., Sánchez, M. and Astrain, D. Object-oriented modeling for the transient performance simulation of parabolic trough collectors using molten salt as heat transfer fluid. Sol. Energy, 95, 192-215 (2013). doi: 10.1016/j.solener.2013.05.015
12. Noureldin, K., Hirsch, T. and Pitz-Paal, R. Virtual Solar Field-Validation of a detailed transient simulation tool for line focus STE fields with single phase heat transfer fluid. Sol. Energy146, 131–140 (2017). doi: 10.1016/j.solener.2017.02.028
13. Noureldin, K. Modelling and Optimization of Transient Processes in Parabolic Trough Power Plants with Single-Phase Heat Transfer Fluid. PhD Dissertation, RWTH Aachen, Aachen (Germany). doi: 10.18154/RWTH-2019-10244 (http://publications.rwth-aachen.de/record/771557)
14. Nouri, B., Noureldin, K., Schlichting, T., Wilbert, S., Hirsch, T., Schroedter-Homscheidt, M., Kuhn, P., Kazantzidis, A., Zarzalejo, L.F., Blanc, P., Fernández, J. and Pitz-Paal, R. Optimization of parabolic trough power plant operation using irradiance maps from all sky imagers. Sol. Energy, 198, 434–453. https://doi.org/10.1016/j.solener.2020.01.045 (accepted)

15. Schroedter-Homscheidt, M., Kosmale, M., Jung, S. and Kleissl, J. Classifying ground-measured 1 minute temporal variability within hourly intervals for direct normal irradiances. Meteorol. Z. (2018). doi: 10.1127/metz/2018/0875.
16. Nouri, B., Wilbert, S., Kuhn, P., Hanrieder, N., Schroedter-Homscheidt, M., Kazantzidis, A., Zarzalejo, L., Blanc, P., Kumar, S., Goswami, N., Shankar, R., Affolter, R. and Pitz-Paal, R. Real-Time Uncertainty Specification of all Sky Imager Derived Irradiance Nowcasts. Remote Sens. 11(9), 1059 (2019) doi: 10.3390/rs11091059
17. Schlichting, T., Bewertung der Verwendbarkeit von Strahlungskarten für den Einsatz in der Regelung eines Parabolrinnensystems, Universität Duisburg-Essen, Master Thesis (2018)
18. Duffie, J. and Beckman, W. Solar Engineering of Thermal Processes, third edition, John Wiley & Sons Hoboken, New Jersey (USA, 2006)